Recognition of (2 S)-Aminomalonyl-Acyl Carrier Protein (ACP) and (2 R)-Hydroxymalonyl-ACP by Acyltransferases in Zwittermicin A Biosynthesis

ARTICLE *in* BIOCHEMISTRY · MARCH 2010

Impact Factor: 3.02 · DOI: 10.1021/bi100141n · Source: PubMed

2 AUTHORS, INCLUDING:

Michael G Thomas
University of Wisconsin–Madison
39 PUBLICATIONS **1,624** CITATIONS

SEE PROFILE

Published in final edited form as:
Biochemistry. 2010 May 4; 49(17): 3667–3677. doi:10.1021/bi100141n.

Recognition of (2*S*)-Aminomalonyl-Acyl Carrier Protein (ACP) and (2*R*)-Hydroxymalonyl-ACP by Acyltransferases in Zwittermicin A Biosynthesis†

Yolande A. Chan and **Michael G. Thomas***
Department of Bacteriology, University of Wisconsin-Madison, 1550 Linden Drive, Madison, WI 53706

Abstract

Polyketide synthases elongate a polyketide backbone by condensing carboxylic acid precursors that are thioesterified to either coenzyme A or an acyl carrier protein (ACP). Two of the three known ACP-linked extender units, (2*S*)-aminomalonyl-ACP and (2*R*)-hydroxymalonyl-ACP, are found in the biosynthesis of the agriculturally important antibiotic zwittermicin A. We previously reconstituted the formation of (2*S*)-aminomalonyl-ACP and (2*R*)-hydroxymalonyl-ACP from the primary metabolites L-serine and 1,3-bisphospho-D-glycerate. In this report we characterize the two acyltransferases involved in the specific transfer of the (2*S*)-aminomalonyl- and (2*R*)-hydroxymalonyl moieties from the ACPs associated with extender unit formation to the ACPs integrated into the polyketide synthase. This work establishes which acyltransferases recognize each extender unit and also provides insight into the substrate selectivity of these enzymes. These are important step towards harnessing these rare polyketide synthase extender units for combinatorial biosynthesis.

Keywords

Polyketide synthase; zwittermicin A; extender unit; aminomalonyl-ACP; hydroxymalonyl-ACP

Polyketides made by bacterial type I polyketide synthases (PKSs) have a wide range of important biological and pharmacological properties including antibacterial, anticancer, antifungal, antiparasitic, and immunosuppressant activities (1,2). The diversity in activities of polyketides is due to the vast structural variations afforded by type I PKS enzymology. These enzymes are large, multidomain complexes that systematically condense thioesterified carboxylic acid precursors into a growing polyketide chain. The first of these precursors to be incorporated is known as the starter unit, while the following precursors that elongate the polyketide backbone are known as extender units. The three enzymatic domains required for a single cycle of chain elongation constitute a minimal module: an acyltransferase (AT), an acyl carrier protein (ACP) and a ketosynthase (KS). The AT transfers an acyl moiety from a starter/extender unit to the 4′-phosphopantetheinyl (4′-Ppant) prosthetic group of a holo-ACP, and chain elongation occurs when the KS catalyzes the decarboxylative condensation of two adjacent ACP-linked thioesters. Additional domains such as a ketoreductase (KR), dehydratase (DH), or enoylreductase (ER) may occur, altering the oxidation state of the β-keto group of the unit. Following completion of the elongation cycles, the acyl chain is cleaved from the PKS by a thioesterase domain, releasing the

†We acknowledge funding by the National Institutes of Health (RO1AI065850).

*CORRESPONDING AUTHOR FOOTNOTE: Phone: 608-263-9075, Fax: 608-262-9865, thomas@bact.wisc.edu

polyketide backbone in either a linear or cyclized form (3). The presence of auxillary domains such as methyltransferases, hydroxylases, halogenases, or glycosyltransferases can result in further modifications to the polyketide (4,5). In addition to the presence/absence of modifying and β-keto processing domains (KR, DH, ER), the type of starter unit and the number and types of extender units greatly add to the extraordinary structural diversity of the polyketides. While there are a plethora of starter units in polyketide biosynthesis (6), there are only eight extender units currently known (7,8).

These extender units can be categorized into two types. The first class includes those that are covalently linked to coenzyme A (CoA): malonyl-CoA, (2*S*)-methylmalonyl-CoA, (2*S*)-ethylmalonyl-CoA, propylmalonyl-CoA, and chloroethylmalonyl-CoA, which incorporate acetyl, propionyl, butyryl, pentanoyl, and chlorobutyryl units, respectively. The second class of extender units includes those that are covalently linked to the 4′-Ppant groups of holo-ACPs: (2*R*)-methoxymalonyl-ACP, (2*S*)-aminomalonyl-ACP, and (2*R*)-hydroxymalonyl-ACP, which elongate a polyketide with methoxyacetyl, glycyl, or glycolyl units, respectively. The first ACP-linked extender unit to be identified, (2*R*)-methoxymalonyl-ACP occurs in the biosynthesis of several polyketides, including the immunosuppressant FK520 (9), the antitumor antibiotic ansamitocin (10), and the antifungal soraphen A (11). Meanwhile, (2*S*)-aminomalonyl-ACP and (2*R*)-hydroxymalonyl-ACP have only been shown to occur in the biosynthesis of the antibiotic zwittermicin A (Figure 1A) (12), although they are proposed as precursors in other biosynthetic pathways (7,13).

Our group is interested in the biosynthesis of zwittermicin A because of its agricultural importance and unusual linear aminopolyol structure (Figure 1A). First isolated from the biocontrol agent *Bacillus cereus* UW85, zwittermicin A has diverse biological activities including broad-spectrum antibiosis against Bacteria and lower Eukarya, plant disease suppression, and enhancement of the insecticidal activity of *Bacillus thuringiensis* toxin against lepidopteran larvae (14-16). In addition, zwittermicin A biosynthesis is an excellent model system to study type I PKSs because it utilizes two rare ACP-linked precursors as well as a CoA-linked precursor (malonyl-CoA) and can thus provide insights into both ACP-linked extender unit biosynthesis and AT domain selectivity for ACP-linked versus CoA-linked extender units.

Although ACP-linked extender units are not as prevalent, these precursors have generated great interest as potential tools for combinatorial biosynthesis because the substituents on the α-carbons (methoxyl, amino, or hydroxyl) provide hydrogen-bonding potential and functionalities not available through the use of the CoA-linked extender units. The heterologous introduction of methoxyl, amino, or hydroxyl groups to a polyketide may enhance the biological or therapeutic activities of the “unnatural” natural product. Furthermore, the addition of amino and hydroxyl groups may provide reactive chemical handles to facilitate downstream semi-synthetic modifications in the generation of even more structural derivatives. The approach of replacing an AT domain of a pathway with a non-cognate AT domain specific for a different extender unit has been used successfully to generate structural derivatives of important polyketides such as FK520 and the erythromycin precursor 6-deoxyerythronolide B (17,18).

As a first step towards exploring (2*S*)-aminomalonyl-ACP and (2*R*)-hydroxymalonyl-ACP as potential tools for combinatorial biosynthesis, we reconstituted the biosynthetic pathways of (2*S*)-aminomalonyl-ACP and (2*R*)-hydroxymalonyl-ACP using heterologously purified enzymes from zwittermicin A biosynthesis (12). In our prior studies of (2*S*)-aminomalonyl-ACP formation, we have shown that ZmaJ covalently tethers L-serine to the 4′-Ppant group of holo-ZmaH, forming seryl-ZmaH, which is subsequently oxidized by ZmaG (NAD^+-dependent) and ZmaI (FAD-dependent) to form (2*S*)-aminomalonyl-ZmaH (Figure 1C). We

also have previously shown that (2*R*)-hydroxymalonyl-ACP formation occurs in an analogous way: ZmaN covalently tethers 1,3-bisphosphoglycerate (1,3-bPG) to the 4′-Ppant group of holo-ZmaD, forming glyceryl-ZmaD; ZmaG and ZmaE (FAD-dependent) then oxidize this intermediate, forming (2*R*)-hydroxymalonyl-ZmaD (Figure 1B).

The next step towards our goal has been to understand how these extender units are incorporated by the producing organism. Based on the structure of zwittermicin A, we previously proposed that it is made by a hybrid nonribosomal peptide synthetase (NRPS) and PKS megasynthase, with PKS modules utilizing (2*S*)-aminomalonyl-ACP and (2*R*)-hydroxymalonyl-ACP extender units to make the glycyl and glycolyl moieties of the molecule (19). Further characterization of the complete biosynthetic gene cluster has revealed that these modules are encoded by two genes: *zmaA*, and *zmaF* (20). ZmaA is a multifunctional enzyme comprised of seven PKS domains and one NRPS component, a condensation (C) domain: KS-KR-ACP-KS-AT-KR-ACP-C (Figure 1B). The first module of ZmaA has been proposed to incorporate (2*S*)-aminomalonyl-ZmaH while the second module has been proposed to incorporate (2*R*)-hydroxymalonyl-ZmaD. The presence of KR domains in each of the modules is consistent with the structure of zwittermicin A, which has hydroxyl groups at C9 and C11 of the glycyl and glycolyl moieties. The absence of an AT domain in the first module of ZmaA suggests that the acyltransferase activity is conferred by a *trans*-acting AT (21); the most likely candidate for providing the function of the “missing” domain is the discrete AT encoded by *zmaF*. Thus, our proposal is that ZmaF transfers the aminomalonyl moiety from (2*S*)-aminomalonyl-ZmaH to the first ACP domain of ZmaA (ZmaA-ACP1) (Figure 1C). We have also proposed that the AT domain of ZmaA (ZmaA-AT) transfers the hydroxymalonyl moiety from (2*R*)-hydroxymalonyl-ZmaD to the second ACP domain of ZmaA (ZmaA-ACP2) (Figure 1D).

To test our hypotheses for (2*S*)-aminomalonyl-ACP and (2*R*)-hydroxymalonyl-ACP incorporation, we heterologously overproduced and purified ZmaF and the excised ZmaA domains ZmaA-ACP1, ZmaA-ACP2, and ZmaA-AT and tested them for activity. Here, we report the characterization of ZmaF and ZmaA-AT, ATs specific for (2*S*)-aminomalonyl-ACP and (2*R*)-hydroxymalonyl-ACP, respectively, in zwittermicin A biosynthesis. This work is the first biochemical characterization of ATs specific for ACP-linked PKS extender units and represents an important step towards harnessing the potential of (2*S*)-aminomalonyl-ACP and (2*R*)-hydroxymalonyl-ACP to generate novel bioactive molecules through combinatorial biosynthesis.

EXPERIMENTAL PROCEDURES

Cloning of zmaF *and the excised* zmaA *domains ZmaA-AT, ZmaA-ACP1, and ZmaA-ACP2*

Standard PCR-based cloning was used to introduce *zmaF* and the *zmaA* gene fragments encoding the excised ZmaA-AT, ZmaA-ACP1, and ZmaA-ACP2 domains into the *E. coli* overexpression vectors pET28b (ZmaF, ZmaA-ACP1, ZmaA-ACP2) or pET30a (ZmaA-AT) (Novagen, Madison, WI). All expression vector clones result in the production of a protein containing an N-terminal histidine tag. Primers used for cloning were: *zmaF* - 5′ AGACATATGAATATTGTATTTATGTTTC 3′ and 5′ AGAAACGTTCTAAAAACTTTTACATTGA 3′; *zmaA-AT* – 5′ GCACCAACCATGGAAGCAACATCAAATAGT 3′ and 5′ TATTTTCTCGAGAGACTACATTGGTAATGGGA 3′; *zmaA-ACP1* – 5′ TTAATAAAATACATATGGCTCAAAGTATAGAA 3′ and 5′ CGTTTCTCGAGTTAAACTTGATTCTTTTGCTT 3′; *zmaA-ACP2* – 5′ CAATTGGAGTCATATGAAATACTGGGAAGAT 3′ and 5′ TTTAGGTTCAGCTCGAGCCTAAACATCAAATT 3′. All clones were verified by sequencing at the University of Wisconsin Biotechnology Sequencing Center.

Heterologous overproduction of proteins

All expression constructs were introduced into *E. coli* BL21 (λDE3). ZmaD, ZmaE, ZmaG, ZmaN, ZmaH, ZmaI, ZmaJ, and Sfp were heterologously overproduced as previously described (22). Cells overproducing ZmaF, ZmaA-AT, ZmaA-ACP1, and ZmaA-ACP2 were grown at 25°C in LB medium containing 50 μg/ml kanamycin. When OD_{600} reached 0.5, the temperature was reduced to 15°C; after 2 h of growth at 15°C, IPTG was added to a final concentration of 60 μ M (or 300 μM for ZmaA-AT). After an additional 16 h growth, cells were harvested by centrifugation.

Purification of proteins

ZmaD, ZmaE, ZmaG, ZmaN, ZmaH, ZmaI, ZmaJ, Sfp, and ZmaA-ACP2 were purified using nickel-affinity chromatography as previously described (22). The same procedure was used to purify ZmaF, ZmaA-AT, and ZmaA-ACP1, with slight modifications. As these proteins required further purification using anion-exchange chromatography, the final step of the nickel-affinity purification was dialysis in low-salt buffer containing 50 mM Tris (pH 8), 50 mM NaCl, and 10% glycerol. Each protein was loaded onto a cartridge containing an anion-exchange resin (ZmaF, BioRad BioScale™ Mini DEAE Affi-Gel Blue; ZmaA-AT, BioRad BioScale™ Mini UNOSphere Q; ZmaA-ACP1, Amersham Q-Trap Sepharose) for further purification. The column was washed with Buffer A (50 mM Tris [pH 8], 50 mM NaCl, and 10% glycerol), and the protein was eluted using a gradient of 0-100% B (50 mM Tris [pH 8], 1M NaCl, and 10% glycerol) (flow rate 3.5 mL/min). Fractions containing ZmaF were pooled and dialyzed in 1 L dialysis buffer (50 mM Tris [pH 8], 100 mM NaCl, and 10% glycerol) at 4°C, concentrated using a Millipore Centriprep protein concentrator, and flash frozen with liquid nitrogen and stored at −80°C. Protein concentrations were determined using the calculated molar extinction coefficients (ZmaF, 37820 $M^{-1}cm^{-1}$; ZmaA-AT, 50810 $M^{-1}cm^{-1}$; ZmaA-ACP1, 15340 $M^{-1}cm^{-1}$; ZmaA-ACP2, 27880 $M^{-1}cm^{-1}$).

Radioactive assays of ZmaF activity with (2S)-aminomalonyl-ZmaH

Reaction mixtures (50 μl) contained the following components: 75 mM Tris (pH 7.5), 10 mM $MgCl_2$, 1 mM TCEP, 500 μM CoA, 1.25 μM ZmaH, 1 μM Sfp, 1 μM ZmaJ, 200 μM NAD^+, 100 μM FAD, 1.5 μM ZmaG, 1.5 μM ZmaI, 3 μM ZmaF, 100 μM L [^{14}C(U)]-L-serine (163 mCi/mmol), and 5 mM ATP. Prior to the addition of ZmaJ, NAD^+, FAD, ZmaG, ZmaI, ZmaF, [^{14}C(U)]-L-serine, and ATP, ZmaH was incubated with Sfp for 1 h at 22°C to become phosphopantetheinylated. The complete reaction was initiated with the addition of ATP, and the reaction was incubated at 22°C for 1.5 h. Control reactions lacking ZmaF, ZmaI, ZmaG, ZmaJ, and ZmaH were performed. Parallel reaction mixtures were set up containing the same components except with 5 μM instead of 1.25 μM ZmaH. An aliquot (30 μL) of the reaction mixtures was removed to tubes containing an equal volume of 2 X cracking buffer (120 mM Tris-HCl pH 6.8, 2% (v/v) β-mercaptoethanol, 1% (w/v) sodium dodecyl sulfate, 25 % (v/v) glycerol, 0.02 % (w/v) bromophenol blue), and 25 μL was loaded onto a 12% polyacrylamide-SDS gel. The gels were stained with Coomassie, destained, dried, exposed to a phosphorimaging screen, and scanned with a Typhoon imager after 4-7 days of exposure. For assaying the misloading of ZmaA-AT by (2S)-aminomalonyl-ZmaH, we followed the same procedure but substituted ZmaA-AT for ZmaF. To quantify the amount of radiolabeled product, a series of ^{14}C standards of known dpm were exposed to a phosphorimaging screen with the SDS-gel of interest. These standards were used to generate a standard curve to correlate pixels to dpm.

Radioactive assays of ZmaF and ZmaA-AT with malonyl-CoA or methylmalonyl-CoA

To address whether ZmaF or ZmaA-AT could recognize malonyl-CoA or methylmalonyl-CoA, reaction mixtures (50 μl) contained the following components: 75 mM Tris (pH 7.5), 10 mM $MgCl_2$, 1 mM TCEP, 2 mM CoA, 1 μM Sfp, 5 μM ZmaA-ACP1 (or ZmaA-ACP2), 5 μM ZmaF (or ZmaA-AT), and 40 μM [^{14}C-C2]-malonyl-CoA (55.2 mCi/mmol) or [^{14}C-C2]-DL-methylmalonyl-CoA (50 mCi/mmol). The complete reaction was initiated by the addition of radiolabeled malonyl-CoA or methylmalonyl-CoA and the reaction was incubated at 22°C for 1.5 h. Prior to the addition of malonyl-CoA or methylmalonyl-CoA, the reaction was incubated at 22°C for 1.0 h to ensure all of the ACPs were in their holo-form. To stop the reaction, 50 μL of 2 X cracking buffer was added to the reaction, and 5 or 10 μL was loaded onto 12% polyacrylamide-SDS gels. The gels were stained with Coomassie, destained, dried, exposed to a phosphorimaging screen, and scanned with a Storm imager after 7-14 days of exposure. Additionally, the proteins bands were cut out of the gels added to scintillation fluid, and the amount of radioactivity present was quantified by scintillation counting.

HPLC analysis of ZmaA-ACP1 and ZmaA-ACP2 reaction products

For assays involving ZmaA-ACP1, reaction mixtures contained the following components: 75 mM Tris (pH 7.5), 10 mM $MgCl_2$, 1 mM TCEP, 50 μM CoA, 12 μM ZmaA-ACP1, 1.25 μM ZmaH, 0.25 μM Sfp, 1 μM ZmaJ, 200 μM NAD^+, 100 μM FAD, 1 μM ZmaG, 1 μM ZmaI, 1 μM ZmaF, 250 μM L-ser, and 5 mM ATP. Prior to the addition of ZmaJ, NAD^+, FAD, ZmaG, ZmaI, ZmaF, L-ser, and ATP, the ACPs ZmaH and ZmaA-ACP1 were allowed to react with Sfp for 1 h at 22°C to become phosphopantetheinylated. The complete reaction was initiated with the addition of ATP, and the reaction was incubated at room 22°C for 45 min. Control reactions lacking ZmaA-ACP1, ZmaH, ZmaJ, ZmaG, ZmaI, ZmaF, and ATP were performed, as were control reactions in which ZmaA-AT replaced ZmaF. Control reactions to determine if either ZmaF or ZmaA-AT loads ZmaA-ACP1 with the hydroxymalonyl moiety of (2*R*)-hydroxymalonyl-ZmaD were also performed and contained the following components: 75 mM Tris (pH 7.5), 10 mM $MgCl_2$, 1 mM TCEP, 500 μM CoA, 12 μM ZmaA-ACP1, 1.25 μM ZmaD, 1 μM Sfp, 1 μM ZmaN, 200 μM NAD^+, 100 μM FAD, 1 μM ZmaG, 1 μM ZmaE, 1 μM ZmaF or ZmaA-AT, 1 U 3-phosphoglycerate phosphokinase (3-PGPK, Sigma), 250 μM 3-phosphoglycerate (3-PG, Sigma), and 5 mM ATP.

For assays involving ZmaA-ACP2, reaction mixtures contained the following components: 75 mM Tris (pH 7.5), 10 mM $MgCl_2$, 1 mM TCEP, 500 μM CoA, 12.5 μM ZmaA-ACP2, 1.25 μM ZmaD, 1 μM Sfp, 1 μM ZmaN, 200 μM NAD^+, 100 μM FAD, 1 μM ZmaG, 1 μM ZmaE, 1 μM ZmaA-AT, 1 U 3-PGPK, 250 μM 3-PG, and 5 mM ATP. Prior to the addition of ZmaN, NAD^+, FAD, ZmaG, ZmaE, ZmaA-AT, 3-PGPK, 3-PG, and ATP, the ACPs ZmaD and ZmaA-ACP2 were allowed to react with Sfp for 1 h at 22°C to become phosphopantetheinylated. The complete reaction was initiated with the addition of ATP, and the reaction was incubated at 22°C for 45 min. Control reactions lacking ZmaA-ACP2, ZmaD, ZmaN, ZmaG, ZmaE, ZmaA-AT, and ATP were performed, as were control reactions in which ZmaF replaced ZmaA-AT. Control reactions to determine if either ZmaA-AT or ZmaF loads ZmaA-ACP2 with the aminomalonyl moiety of (2*S*)-aminomalonyl-ZmaH were also performed and contained the following components: 75 mM Tris (pH 7.5), 10 mM $MgCl_2$, 1 mM TCEP, 500 μM CoA, 12.5 μM ZmaA-ACP2, 1.25 μM ZmaH, 1 μM Sfp, 1 μM ZmaN, 200 μM NAD^+, 100 μM FAD, 1 μM ZmaG, 1 μM ZmaI, 1 μM ZmaA-AT or ZmaF, 250 μM L-ser, and 5 mM ATP.

For assays involving ZmaA-AT, ZmaA-ACP2, and the addition of methylmalonyl-CoA or malonyl-CoA as a substrate, reaction mixtures contained the following components: 75 mM

Tris (pH 7.5), 10 mM $MgCl_2$, 1 mM TCEP, 500 μM CoA, 12.5 μM ZmaA-ACP2, 1.25 μM ZmaD, 1 μM Sfp, 1 μM ZmaN, 200 μM NAD^+, 100 μM FAD, 1 μM ZmaG, 1 μM ZmaE, 1 μM ZmaA-AT, 1 U 3-PGPK, 5 mM ATP, and 100 μM malonyl-CoA or DL-methylmalonyl-CoA. Prior to the addition of ZmaN, NAD^+, FAD, ZmaG, ZmaE, ZmaA-AT, 3-PGPK, ATP, and malonyl-CoA or methylmalonyl-CoA, the ACPs ZmaD and ZmaA-ACP2 were allowed to react with Sfp for 1 h at 22°C to become phosphopantetheinylated. The complete reaction was initiated with the addition of malonyl-CoA or methylmalonyl-CoA, and the reaction was incubated at 22°C for 45 min. To generate malonyl-ZmaA-ACP2 and methylmalonyl-ZmaA-ACP2 standards, CoA was not added to the reaction mixtures so that the only source of substrate for Sfp was malonyl-CoA or methylmalonyl-CoA.

HPLC analysis of reaction products was performed with Vydac (Hesperia, CA) C8 (for ZmaA-ACP1 only) and C18 (for ZmaA-ACP1 and ZmaA-ACP2) peptide columns (250 X 4.6 mm). Reaction products were separated using a 20-80% acetonitrile/0.1% TFA gradient over 20 min at a flow rate of 1 mL/min. The elution of proteins was monitored at A_{220}. ZmaA-ACP1 and ZmaA-ACP2 were collected as they eluted from the HPLC, flash-frozen, and lyophilized prior to MALDI-TOF MS analysis. For analysis of malonyl-ZmaA-ACP2 or methylmalonyl-ZmaA-ACP2 formation, elution times were compared to enzymatically generated standards.

MALDI-TOF MS analysis of ZmaA-ACP1 and ZmaA-ACP2 reaction products

Lyophilized samples were resuspended in double-distilled water and added to the sinipinic acid matrix (10 mg/L in 50% acetonitrile/0.05% TFA). MALDI-TOF MS analysis was performed using a Voyager Biospectrometry Workstation (DE-Pro; Applied Biosystems, Foster City, CA) in linear, positive-ion mode. The instrument was calibrated using cytochrome C, apomyoglobin, and aldolase (Sigma) as standards.

ESI-MS analysis of ZmaA-ACP1 reactions lacking ZmaG and ZmaI

Lyophilized samples to be analyzed were prepared as described above and were submitted to the Mass Spectrometry Facility at the University of Wisconsin Biotechnology Center. Samples were analyzed using a Thermo Scientific LTQ Orbitrap XL system.

RESULTS AND DISCUSSION

Purification of ZmaF and the excised domains ZmaA-ACP1, ZmaA-ACP2, and ZmaA-AT

As shown in Figure 1B, we have proposed that ZmaF is a stand-alone AT domain that catalyzes the transfer of (2*S*)-aminomalonate from (2*S*)-aminomalonyl-ZmaH to the first ACP domain of ZmaA (ZmaA-ACP1). Additionally, we have proposed that the AT domain of ZmaA (ZmaA-AT) catalyzes the transfer of (2*R*)-hydroxymalonate from (2*R*)-hydroxymalonyl-ZmaD to the second ACP domain of ZmaA (ZmaA-ACP2) (Figures 1B-D). We decided to take a biochemical approach to test these hypotheses. To accomplish this, we first needed to obtain purified proteins. We cloned *zmaF* and the regions of *zmaA* corresponding to ZmaA-ACP1, ZmaA-ACP2, and ZmaA-AT into *Escherichia coli* overexpression vectors and purified the resultant N-terminally histidine-tagged proteins. ZmaF was purified to near homogeneity using nickel-affinity and ion-exchange chromatography. To excise the ACP domains from ZmaA, we analyzed the linker regions flanking the domains of interest, and we used multiple sets of primers to generate constructs with no linkers or with linkers of various lengths. For ZmaA-ACP1, only two of the eight constructs resulted in overproduced protein; of these, most were insoluble or sparingly soluble. The construct that resulted in the highest level of soluble protein was selected for our analysis. This construct contained 70 amino acids of the N-terminal linker and 9 amino acids of the C-terminal linker. ZmaA-ACP1 was purified by nickel-affinity chromatography,

with an additional purification by ion-exchange chromatography as needed. The use of an additional step in purification was needed periodically due to the observation that ZmaA-ACP1 preparations varied in their level of protein production and solubility. An overexpression construct resulting in the production of ZmaA-ACP2 containing both N-terminal and C-terminal linkers in their entirety led to overproduced protein that was highly soluble. After purification using nickel-affinity chromatography, no further purification was necessary. Although excised AT domains from modular megasynthases are notorious for being insoluble (23), we were nonetheless motivated to attempt to excise ZmaA-AT. A construct we made containing most of the N-terminal linker (92 amino acids) and a small portion (13 amino acids) of the C-terminal linker resulted in overproduced, soluble protein, which was purified by nickel-affinity and anion-exchange chromatography.

We also note that we initially attempted to characterize full-length ZmaA, which was heterologously overproduced in *E. coli* with an N-terminal histidine tag; however, due to its large size (379 kDa), ZmaA was produced in relatively small amounts and was difficult to purify. Furthermore, partially purified protein preparations of ZmaA were subject to degradation, as determined by SDS-PAGE analysis. By utilizing the excised domains, we were able to circumvent the difficulties of working with an unstable and partially pure protein. This approach also facilitated the characterization of the moieties attached to the active sites of the ACPs and ZmaA-AT using mass spectrometry, as discussed later.

Formation of a (2S)-aminomalonyl-ZmaF enzyme intermediate

ATs specific for CoA-linked substrates have been the focus of numerous investigations in polyketide and fatty acid biosynthesis. While they may differ in whether they are discrete enzymes or *cis*-acting domains of a multimodular complex, these enzymes utilize a common two-step mechanism to transfer the acyl groups of acyl-CoAs to their recipient ACPs. In the first step, the AT transfers the acyl group from an acyl-CoA substrate to an active site serine, forming an acyl-*O*-enzyme intermediate while releasing CoASH. In the next step, the acyl group on the AT is transferred to the 4′-Ppant prosthetic group of a recipient holo-ACP, forming an acyl-ACP product (24,25)].

To date, there has been no biochemical characterization of any ATs specific for ACP-linked extender units, although there is genetic evidence from domain replacement experiments supporting the role of one of these ATs in the incorporation of (2*R*)-methoxymalonyl-ACP in FK520 biosynthesis (17,26)]. Based on our sequence analysis of ZmaF, which contains the conserved active site motif GXSXG, it seemed likely that ZmaF utilizes a mechanism analogous to that observed for ATs specific for CoA-linked substrates. We propose that in the first step of the reaction, ZmaF transfers the aminomalonyl moiety of (2*S*)-aminomalonyl-ZmaH to the ZmaF active site serine, forming a (2*S*)-aminoacyl-ZmaF intermediate.

To test whether a covalently linked intermediate is formed, we performed radioactive transacylase assays using [^{14}C]-(2*S*)-aminomalonyl-ZmaH and looked for the formation of a ZmaF-linked intermediate using SDS-PAGE followed by phosphorimaging. For our complete reaction, we incubated ZmaF with the components necessary for [^{14}C]-(2*S*)-aminomalonyl-ZmaH formation ([^{14}C]-L-serine, holo-ZmaH, ZmaJ, ZmaG, ZmaI, NAD^+, FAD, and ATP). For our controls, we set up parallel reactions lacking ZmaF, ZmaI, ZmaG, ZmaJ, or ZmaH. As shown in Figure 2A, ZmaF becomes radiolabeled when all the components for (2*S*)-aminomalonyl-ZmaH are present in the reaction mixture. Quantifying the amount of radiolabeled ZmaF in a typical experiment as shown in Figure 2 determined that only 0.4% of the total ZmaF was radiolabeled (0.6 pmol of radiolabeled ZmaF of 150 pmol of total ZmaF added to the reaction). It is not clear at this point why such a low level of labeling was observed. One possibility was the low level of substrate ([2*S*]-

aminomalonyl-ZmaH). ZmaH was present at only 1 μM, setting a maximum concentration of (2*S*)-aminomalonyl-ZmaH at 1 μM. Additionally, we have previously shown that the K_m of ZmaJ for L-serine is 1.8 mM (12). Due to limitations in the specific activity of radiolabeled L-serine, this substrate was added at more than 10-fold lower than the Km. This may also impact the level of (2*S*)-aminomalonyl-ZmaH in the reaction. Alternatively, the radiolabeled intermediate may not be stable under these assay conditions and the (2*S*)-aminomalonyl group is being hydrolyzed from ZmaF. An additional observation was that a longer exposure of the gel shown in Figure 2A, and other equivalent gels, to the phosphorimager plate detected a very low level of radiolabeled ZmaF in the reaction lacking ZmaI (0.17 pmol of radiolabeled ZmaF). This suggests that ZmaF weakly recognizes the product of the ZmaG reaction, either 2-amino-3-oxopropionyl-ZmaH or 2-amino-3,3-dihydroxypropionyl-ZmaH.

To further investigate the potential transfer of an intermediate of the (2*S*)-seryl-ZmaH to (2*S*)-aminomalonyl-ZmaH conversion, we repeated the labeling experiments with an almost five-fold higher concentration of ZmaH (1.25 μM compared to 5 μM). The goals were to determine whether an increase in the concentration of the ZmaF substrate, (2*S*)-aminomalonyl-ZmaH, increased (2*S*)-aminomalonyl-ZmaF formation, and whether other intermediates were also competent for acylation of ZmaF when the ZmaH concentration was increased. Under these assay conditions, an approximately 2-fold higher level of (2*S*)-aminomalonyl-ZmaF was detected (1.3 pmol at 5 μM ZmaH versus 0.6 pmol at 1.25 μM ZmaH) (Figure 2B). Additionally, it was clearly evident that ZmaF was also radiolabeled in two of the control reactions, those lacking ZmaI or ZmaG (Figure 2B). In a reaction lacking ZmaI, the aldehyde [^{14}C]-2-amino-3-oxopropionyl-ZmaH is formed instead of [^{14}C]-(2*S*)-aminomalonyl-ZmaH. In aqueous reaction buffer, this aldehyde is likely to interconvert between this species and the geminal diol [^{14}C]-2-amino-3,3-dihydroxypropionyl-ZmaH. While it is possible that either of these may be recognized by ZmaF, we propose that ZmaF is more likely to recognize and become misacylated by the latter, as it closely resembles (2*S*)-aminomalonyl-ZmaH, differing only in the oxidation state of a single oxygen atom. ZmaF clearly prefers (2*S*)-aminomalonyl-ZmaH over (2*S*)-amino-3-oxopropionyl-ZmaH based on the lower level of ZmaF labeling that was observed (0.7 pmol of [2*S*]-amino-3-oxopropionyl-ZmaF versus 1.3 pmol of [2*S*]-aminomalonyl-ZmaF). In the control reaction lacking ZmaG, radiolabeling of ZmaF was also evident under these assay conditions. In contrast, when ZmaH levels were lower, no ZmaF labeling was detected at even after an extended exposure of the gel to the phosphorimaging screen. This suggests that when ZmaH levels are higher, ZmaF recognizes (2*S*)-seryl-ZmaH and forms a (2*S*)-seryl-ZmaF intermediate, albeit at lower levels (0.4 pmol total) than seen in the complete reaction (1.3 pmol) and the reaction lacking ZmaI (0.7 pmol). The remaining control reactions lacking either ZmaF, ZmaJ, or ZmaH all failed to result in radiolabeling of ZmaF. Thus, the formation of an acyl-ZmaH intermediate was essential for self-acylation by ZmaF. We also note that we tested whether ZmaF will recognize [^{14}C]-malonyl-CoA or [^{14}C]-(2*S*)-methylmalonyl-CoA under these assay conditions to form the respective acyl-ZmaF intermediate. Neither of these extender units were substrates for ZmaF. All of these data are consistent with our proposal that ZmaF recognizes (2*S*)-aminomalonyl-ZmaH as its preferred substrate and forms a (2*S*)-aminomalonyl-ZmaF intermediate.

At the higher concentration of ZmaH, differences in the level of detectable radiolabeling of ZmaH were also noted (Figure 2B). In the absence of ZmaJ or ZmaH, no radiolabel was evident as expected. For the complete reaction and the reactions lacking ZmaF, ZmaI, or ZmaG, radiolabeling of ZmaH was clearly evident, but it occurred at variable levels. In the reaction lacking ZmaG, the progression of (2*S*)-aminomalonyl-ZmaH formation is stalled at (2*S*)-seryl-ZmaH, as we have shown previously (12). This appeared to be the most stable acyl-ZmaH product based on this reaction resulting in the highest detectable level of

radiolabeling of ZmaH (1.7 pmol detected). Interestingly, when the next enzyme in (2*S*)-aminomalonyl-ZmaH formation, ZmaI, was excluded from the reaction, the amount of radiolabeled ZmaF decreased to only 0.2 pmol. The product at this point in the pathway is [^{14}C]-2-amino-3-oxopropionyl-ZmaH and is clearly less stable under these assay conditions. The same is true for the reaction lacking ZmaF in which the (2*S*)-aminomalonyl-ZmaH intermediate that accumulates is not as stable as (2*S*)-seryl-ZmaH (0.3 pmol versus 1.7 pmol, respectively). Finally, when the reaction contains all of the enzymes for the formation of (2*S*)-aminomalonyl-ZmaF, the amount of radiolabel on ZmaF is 0.5 pmol, approximately 2-fold higher than seen in the absence of ZmaF. These results suggest that each of the intermediates has a different level of stability while tethered to the ZmaH. One possible explanation for this may be different affinities of these intermediates for the cleft between helices 2 and 3 of ACPs (27). This cleft has been hypothesized to sequester acyl intermediates in fatty acid biosynthesis and stabilize them between rounds of synthesis. Interestingly, the (2*S*)-aminoacyl-ZmaH intermediate is more stable in the presence of ZmaF, suggesting the interactions between the AT and ACP partners influence the stability of the acyl-ACP intermediate.

ZmaF catalyzes transfer of the (2S)-aminomalonyl moiety to ZmaA-ACP1

The analysis of ZmaF discussed above provided evidence that ZmaF is able to catalyze the first half reaction of its AT activity. To determine if ZmaF catalyzes the second step, the transfer of the aminomalonyl moiety from its active site serine to the 4′-Ppant group of ZmaA-ACP1, we used an HPLC-based assay combined with MALDI-TOF MS analysis. Like the other ACPs we have overproduced in *E. coli* (12), ZmaA-ACP1 was purified as being predominantly in the inactive, apo-form (Figure 3, trace A; Table 1). To convert ZmaA-ACP1 to the active, holo- form, we incubated it with CoA and the 4′-Ppant transferase Sfp. HPLC and MALDI-TOF MS analysis determined that the majority of ZmaA-ACP1 was now holo-ZmaA-ACP1 (Figure 3, trace B; Table 1). Because ZmaA-ACP1 was capable of being modified by Sfp, we were encouraged that the excised ACP was likely folded correctly. To investigate whether ZmaF can transfer the (2*S*)-aminomalonyl moiety from (2*S*)-aminomalonyl-ZmaH to ZmaA-ACP1, we incubated ZmaF, holo-ZmaA-ACP1, and the enzymes required for (2*S*)-aminomalonyl-ZmaH formation (holo-ZmaH, ZmaJ, ZmaG, and ZmaI), initiating the reaction with ATP. HPLC analysis of the complete reaction using a C18 peptide column resulted in the detection of two distinct ZmaA-ACP1-associated products (Figure 3, trace D). Based on elution time and MS analysis, one of these products was holo-ZmaA-ACP1 that had not been acylated. The second product eluted earlier than holo-ZmaA-ACP1 and was absent in a reaction lacking ZmaF, in which only holo-ZmaA-ACP1 was detected (Figure 3, compare traces C and D). Mass spectrometry of this product of the complete reaction demonstrated that it had a mass consistent with glycyl-ZmaA-ACP1, the decarboxylated form of (2*S*)-aminomalonyl-ZmaA-ACP1. The detection of the decarboxylated product is not surprising, based on our previous work in which we consistently detected glycyl-ZmaH, the decarboxylated form of (2*S*)-aminomalonyl-ZmaH when using MALDI-TOF MS analysis (12). Under similar reaction conditions, (2*S*)-aminomalonyl-ZmaA-ACP1 is predicted to spontaneously decarboxylate, and the formation of glycyl-ZmaA-ACP1 is indicative of the formation of (2*S*)-aminomalonyl-ZmaA-ACP1.

Because ZmaA-ACP1 adheres strongly to the C18 peptide column, we were required to thoroughly flush the column and perform multiple injections with water between samples to eliminate carryover. To facilitate our analysis, we switched to a C8 peptide column and performed these assays in the same manner. While this minimized our efforts in cleaning the column between runs, the C8 peptide column did not separate glycyl-ZmaA-ACP1 from holo-ZmaA-ACP1 as well as the C18. Nonetheless, MALDI-TOF MS analysis enabled us to distinguish between the different ZmaA-ACP1 species. Using this new column, control

reactions lacking holo-ZmaA-ACP1, holo-ZmaH, ZmaJ, ZmaG, ZmaI, or ZmaF were analyzed. Only in the presence of all the enzymes did we observe a product with a mass consistent with glycyl-ZmaA-ACP1. Our control reactions lacking holo-ZmaH, ZmaJ, ZmaG, and ZmaF resulted in products with masses corresponding to holo-ZmaA-ACP1. Interestingly, in the control reaction lacking ZmaI, we observed two products; MALDI-TOF and ESI MS analysis revealed a major peak with a mass corresponding to holo-ZmaA-ACP1 and a minor peak with a mass 88 Da larger than holo-ZmaA-ACP1 (Table 1). We propose that this minor peak corresponds to 2-amino-3-oxopropionyl-ZmaA-ACP1. This species could arise from the ZmaF-catalyzed incorporation of either the aldehyde 2-amino-3-oxopropionyl-ZmaH or the geminal diol 2-amino-3,3-dihydroxypropionyl-ZmaH; incorporation of the latter would yield 2-amino-3,3-dihydroxypropionyl-ZmaA-ACP1, which would likely convert to the aldehyde 2-amino-3-oxopropionyl-ZmaA-ACP1 under our acidic assay conditions. Based on the structural similarity between the true substrate (2*S*)-aminomalonyl-ZmaH and the geminal diol 2-amino-3,3-dihydroxypropionyl, we propose that the second scenario is more probable. Consistent with the radiolabeling studies, detection of this product occurred with a higher concentration of ZmaH relative to ZmaF. Thus, ZmaF is able to transfer the incorrect substrate, albeit at a much lower efficiency than (2*S*)-aminomalonate. We also note that while we were able to detect the formation of seryl-ZmaF, we were unable to detect ZmaF-catalyzed formation of seryl-ZmaA-ACP1. This may be due to the failure of ZmaF to catalyze this reaction or the level of activity is below our detection limit. The former possibility is intriguing because this may suggest that the ZmaF is able to discriminate between substrates after formation of the acyl-ZmaF intermediate. Additional support for this aspect of transacylation will be discussed below.

As shown in Figure 3, a reaction containing ZmaF, holo-ZmaA-ACP1, and (2*S*)-aminomalonyl-ZmaH results in a mixture of glycyl-ZmaA-ACP1 and holo-ZmaA-ACP1. Despite our attempts to optimize the reaction conditions by varying enzyme concentrations or incubation times, we consistently observed only partial conversion to glycyl-ZmaA-ACP1. Reactions in which we pre-formed seryl-ZmaH prior to the addition of ZmaG, ZmaI, and ZmaF also resulted in a mixture of species. It seems unlikely that the partial conversion was due to insufficient amounts of (2*S*)-aminomalonyl-ZmaH, because our previous work demonstrated it readily forms under similar reaction conditions (12). Furthermore, we observed that the relative amounts of glycyl-ZmaA-ACP1 and holo-ZmaA-ACP1 varied, depending on the preparation of ZmaA-ACP1. In light of the difficulties in obtaining soluble and pure protein, one possible explanation is that our preparations contain a mixed population of ZmaA-ACP1, some that is folded properly and some that is slightly misfolded but still competent for modification by Sfp. This misfolded protein, however, may not be competent for docking with ZmaF. We note that for a particular protein preparation, the same level of acylated versus nonacylated ZmaA-ACP1 was observed regardless of whether the enzyme concentrations were varied, the time of incubation was changed, or the time between the termination of the reaction and injection of the HPLC varied. Thus, it appears that only a certain population of ZmaA-ACP1 was competent for acylation. To date, we have been unable to separate these populations of ZmaA-ACP1 using chromatographic techniques.

Another explanation for the incomplete conversion is that ZmaF may not dock as well with its cognate ACP when it is excised from ZmaA, and thus, our *in vitro* assays may be lacking structural components that are important for this interaction. We propose that one of these elements might be a cryptic AT domain located in the interdomain region between the first KS and KR domains of ZmaA. Cryptic AT domains, lacking the active site GXSXG motifs found in functional AT domains, are found in modules with “missing” AT domains and are proposed to assist in the docking of *trans*-AT proteins to the PKS (28,29). The relatively large size of the interdomain region (~390 residues) between the first KS and KR domains

of ZmaA suggests that it may have a role as a docking site for ZmaF. To investigate the potential involvement of a cryptic AT domain, we cloned this interdomain region into an overexpression vector and purified the resultant hexa-histidine tagged protein. Adding this protein to our assays had no effect on the formation of glycyl-ZmaA-ACP1. Furthermore, no interactions between this interdomain region and ZmaF or ZmaA-ACP1 were detected by native gel electrophoresis. The finding that this excised interdomain region did not enhance the formation of glycyl-ZmaA-ACP1 *in vitro* or result in detectable interactions with ZmaF or ZmaA-ACP1, however, does not eliminate the possibility that it may have a docking role as part of a full-length module *in vivo*. The assay for detecting the incorporation of (2S)-aminomalonyl-ZmaH requires multiple proteins (Sfp, ZmaH, ZmaJ, ZmaG, ZmaI, ZmaF, and the excised domain ZmaA-ACP1) and several enzymatic conversions. Although we were not able to achieve full acylation of holo-ZmaA-ACP1 by ZmaF in this *in vitro* assay, our HPLC and mass spectral data support the role of ZmaF as an AT involved in incorporating (2*S*)-aminomalonyl-ZmaH.

ZmaA-AT catalyzes the transfer of the (2R)*-hydroxymalonyl moiety to ZmaA-ACP2*

Like ZmaF, ZmaA-AT contains the conserved active site motif GXSXG characteristic of ATs. We proposed that ZmaA-AT utilizes a similar catalytic mechanism, transferring the hydroxymalonyl moiety from (2*R*)-hydroxymalonyl-ZmaD to ZmaA-ACP2 in a two-step process. In the first step, ZmaA-AT transfers the hydroxymalonyl moiety of (2*R*)-hydroxymalonyl-ZmaD to its active site serine, forming an acyl-ZmaA-AT intermediate. We wanted to use a radioactive assay to monitor the formation of this intermediate, analogous to our analysis of ZmaF; however, attempts to procure radioactive precursors to the substrate 1,3-bPG from two different companies were unsuccessful. As an alternative approach to detecting the acylation of ZmaA-AT, we used mass spectrometry to determine whether the mass of ZmaA-AT changed when incubated with (2*R*)-hydroxymalonyl-ZmaD. Analysis of the full-length ZmaA-AT proved problematic, so we attempted to detect mass change associated with the conserved catalytic serine residue by using trypsin digestion followed by mass spectrometry. We analyzed two samples, one containing ZmaA-AT and another containing ZmaA-AT plus (2*R*)-hydroxymalonyl-ZmaD. Unfortunately, while we were able to detect every other fragment of ZmaA-AT, multiple attempts using trypsin digestion or other proteases to detect the peptide fragment containing the conserved serine were unsuccessful for either sample. Thus, some aspect of this region of ZmaA-AT makes it unamenable to this type of analysis.

Since we could not use radiolabeling or mass spectrometry to analyze the first half-reaction of ZmaA-AT, we focused our attention on whether we could detect the complete ZmaA-AT reaction. We performed HPLC-based assays followed by MALDI-TOF MS analysis to determine whether (2*R*)-hydroxymalonate could be transferred from (2*R*)-hydroxymalonyl-ZmaD to ZmaA-ACP2. Like ZmaA-ACP1, the excised domain was purified from *E. coli* as being mostly in the apo-form. Incubation with CoA and Sfp resulted in the nearly complete conversion to the holo- form, as determined by HPLC and MALDI-TOF MS (Figure 4, traces A and B; Table 2). To investigate whether ZmaA-AT can transfer the hydroxymalonyl moiety from (2*R*)-hydroxymalonyl-ZmaD to ZmaA-ACP2, we incubated ZmaA-AT, holo-ZmaA-ACP2, and the enzymes required for (2*R*)-hydroxymalonyl-ZmaD formation (holo-ZmaD, ZmaN, ZmaG, and ZmaE), initiating the reaction with ATP, which is required by the kinase that converts 3-phosphoglycerate to the glycolytic substrate 1,3-bPG. A control reaction lacking ZmaA-AT was also run to monitor whether modification of ZmaA-ACP2 was dependent upon ZmaA-AT. The holo-ZmaA-ACP2 in the reaction lacking ZmaA-AT was unmodified, based on the observation that ZmaA-ACP2 eluted with a retention time consistent with holo-ZmaA-ACP2 (Figure 4, trace C) and had a mass consistent with the holo- form of the ACP (Table 2). Analysis of holo-ZmaA-ACP2 in the

presence of all the enzymes needed for (2*R*)-hydroxymalonyl-ZmaD formation and ZmaA-AT found that the protein eluted earlier, with a slight broadening of the total time of elution, relative to the control reaction lacking ZmaA-AT (Figure 4, trace D). MALDI-TOF MS analysis of this collected peak revealed a mass consistent with glycolyl-ZmaA-ACP2, the decarboxylated form of (2*R*)-hydroxymalonyl-ZmaA-ACP2 (Table 2). These data demonstrated that the observed change to holo-ZmaA-ACP2 in the complete reaction was ZmaA-AT-dependent and not due to the acylation of the ACP by ZmaN or a modification by any other enzymes in the reaction mixture.

Control reactions lacking each of the components (holo-ZmaA-ACP2, holo-ZmaD, ZmaN, ZmaG, and ZmaE) were analyzed by HPLC (Supporting Information Figure S1) and MALDI-TOF MS. Only in the presence of all the enzymes did we observe an eluting product with a mass consistent with glycolyl-ZmaA-ACP2. To provide additional evidence that this change did not arise from the direct acylation of holo-ZmaA-ACP2 by ZmaN, we incubated holo-ZmaA-ACP2, ZmaN, and 1,3-bPG and analyzed the reaction using HPLC (Figure S1) and MALDI-TOF MS. Only a mass consistent with holo-ZmaA-ACP2 was observed, supporting the notion that the formation of glycolyl-ZmaA-ACP2 is due to the ZmaA-AT-catalyzed transfer of the hydroxymalonyl moiety from (2*R*)-hydroxymalonyl-ZmaD. Also, we note that in contrast to ZmaF, ZmaA-AT did not appear to transfer the product of the ZmaG-catalyzed reaction product, 2-hydroxy-3,3-dihydroxypropionyl-ZmaD. While we cannot eliminate the possibility that the amount transferred is below the detection limit of our assays, our results suggest that relative to ZmaF, ZmaA-AT is more selective for the fully oxidized carboxylic acid moiety of the substrate. We also note that we did not detect any acylation of ZmaA-ACP2 when malonyl-CoA or (2*S*)-methylmalonyl-CoA replaced (2*R*)-hydroxymalonyl-ACP in the reaction mixtures, and we did not detect acylation of ZmaA-AT when this enzyme was incubated with [^{14}C]-malonyl-CoA or [^{14}C]-(2*S*)-methylmalonyl-CoA. This suggests that ZmaA-AT does not recognize these extender units.

Substrate specificities of ZmaF and ZmaA-AT

Our data clearly demonstrate that ZmaF transfers the aminomalonyl moiety from (2*S*)-aminomalonyl-ZmaH to ZmaA-ACP1 while ZmaA-AT transfers the hydroxymalonyl moiety from (2*R*)-hydroxymalonyl-ZmaD to ZmaA-ACP2. As described above, we also determined that neither ZmaF nor ZmaA-AT recognizes malonyl-CoA or (2*S*)-methylmalonyl-CoA. To further probe the specificity of ZmaF for an alternative ACP-linked extender unit, we performed HPLC-based assays followed by MALDI-TOF MS analysis. When we analyzed a reaction containing ZmaF, (2*S*)-aminomalonyl-ZmaH, and holo-ZmaA-ACP2, we observed that ZmaA-ACP2 eluted with a retention time and mass corresponding to holo-ZmaA-ACP2, not the acylated form. Experiments performed with ZmaF, (2*R*)-hydroxymalonyl-ZmaD, and either holo-ZmaA-ACP1 or holo-ZmaA-ACP2 resulted in the detection of ACPs with elution times and masses corresponding to the holo-forms of these excised ACPs and not the acylated forms. These results are consistent with our proposal that ZmaF is the discrete AT for the first PKS module of ZmaA containing ACP1 and not the second module of ZmaA containing ACP2. Using a similar approach, we also investigated the specificity of ZmaA-AT. A reaction containing ZmaA-AT, (2*R*)-hydroxymalonyl-ZmaD, and holo-ZmaA-ACP1 was analyzed and resulted in an ACP with an HPLC elution time and a mass consistent with holo-ZmaA-ACP1. Assays performed with ZmaA-AT, (2*S*)-aminomalonyl-ZmaH and either holo-ZmaA-ACP1 or holo-ZmaA-ACP2 resulted in the detection of the excised holo- ACPs, not their acylated forms. These data further support our proposal that ZmaA-AT incorporates (2*R*)-hydroxymalonyl-ZmaD by transferring the hydroxymalonyl moiety to the second ACP domain of ZmaA. It is important to note that our assays investigating the acylation of ZmaA-ACP1 and ZmaA-ACP2 by

noncognate AT domains used concentrations of the ACPs that are likely to be far below the anticipated K_d of these noncognate AT/ACP interactions. Thus, it is not surprising that cross-talk between the AT/ACP systems was not detected under our assay conditions. Regardless, these data are consistent with our conclusion that the correct AT/ACP pairs have been identified.

While our MALDI-TOF MS data suggested that ZmaA-AT under our assay conditions does not transfer the (2*S*)-aminomalonyl moiety from (2*S*)-aminomalonyl-ZmaH to either ZmaA-ACP1 or ZmaA-ACP2 and ZmaF does not transfer the (2*R*)-hydroxymalonyl moiety to either ZmaA-ACP1 or ZmaA-ACP2, these experiments would require both half reactions of the ATs to occur. We were interested in determining whether the ATs showed different selectivities for the first half reaction when incubated with the alternative ACP-linked extender unit. Due to limitations in radiolabeled substrate availability and mass spectrometry, we could only address whether the ZmaA-AT would recognize (2*S*)-aminomalonyl-ZmaH and form a (2*S*)-aminomalonyl-ZmaF intermediate. We were unable to investigate whether ZmaF can acylate itself with (2*R*)-hydroxymalonate from ZmaD.

To investigate whether ZmaA-AT could form the incorrect (2*S*)-aminomalonyl-ZmaA-AT intermediate, we used [^{14}C]-(2*S*)-aminomalonyl-ZmaH as the substrate and monitored acylation of ZmaA-AT by SDS-PAGE in combination with phosphorimaging. After ZmaA-AT was incubated with [^{14}C]-(2*S*)-aminomalonyl-ZmaH (final concentration of ZmaH was 1 μM), we did not detect acylation of ZmaA-AT when 1 μM of ZmaH was included in the reaction mixture. In contrast, when the concentration of ZmaH was raised to either 3 μM or 5 μM, acylation of ZmaA-AT was clearly evident, but only when [^{14}C]-(2*S*)-aminomalonyl-ZmaH was formed (Figure 5). Reactions lacking any of the (2*S*)-aminomalonyl-ZmaH biosynthetic enzymes did not result in detectable levels of acyl-ZmaA-AT product. This is in contrast to ZmaF, which recognized not (2*S*)-aminomalonate, but also L-serine and (2*S*)-2-amino-3-oxopropionate. The level of acyl-ZmaA-AT formation (0.4 pmol) with 5 μM ZmaH was comparable to what was observed when ZmaF was incubated with only 1 μM ZmaH (0.6 pmol). Additionally, the same pattern and level of radiolabeled ZmaH was detected as observed when ZmaF was incubated with 5 μM ZmaH, further supporting that there are varying levels of stability of the ZmaH-linked intermediates during (2*S*)-aminomalonyl-ZmaH formation.

Interestingly, while a covalent (2*S*)-aminomalonyl-ZmaA-AT intermediate was detected, we did not detect the transfer of the (2*S*)-aminomalonyl moiety to either ZmaA-ACP1 or ZmaA-ACP2 using HPLC assays that used either 1 or 5 μM ZmaH. This observation, in combination with the observation that ZmaF formed a seryl-ZmaF intermediate but did not transfer the seryl group to ZmaA-ACP1, suggests a model by which the second half-reaction of AT domains may be selective for the correct acyl-linked intermediate. Two reasons for the inability ZmaA-AT to transfer the (2*S*)-aminomalonyl group may be the altered stereochemistry of the substrate or that the hydroxyl group at C2 has been replaced by an amino group. These data suggest that more analysis must be done on the second half-reaction of AT domains.

Conclusions

This work contributes to our understanding of the biosynthesis of an agriculturally important molecule and represents the first biochemical characterization of ATs specific for ACP-linked extender units. We have demonstrated that the discrete enzyme ZmaF is a *trans*-acting AT that is involved in the incorporation of (2*S*)-aminomalonyl-ACP, transferring the aminomalonyl moiety from (2*S*)-aminomalonyl-ZmaH to the first ACP domain of ZmaA. We also have shown that the excised *cis*-acting AT domain from ZmaA incorporates (2*R*)-hydroxymalonyl-ACP, transferring the hydroxymalonyl moiety from (2*R*)-hydroxymalonyl-

ZmaD to the second ACP domain of ZmaA. Preliminary analysis of the substrate specificity of these AT domains suggests the second half-reaction of these domains are selective for the correct acyl-AT intermediate. These PKS extender units hold enormous potential as tools for combinatorial biosynthesis because the substituents on their α-carbons confer functionalities not available through the use of the other known extender units; the incorporation of these extender units introduces amino or hydroxyl groups, which offer hydrogen-bonding potential and chemically reactive handles for downstream semi-synthetic modifications. The characterization of the enzymes involved in incorporating (2*S*)-aminomalonyl-ACP and (2*R*)-hydroxymalonyl-ACP sets the stage for engineering natural product biosynthetic pathways to utilize these precursors for the generation of novel bioactive molecules.

Supplementary Material

Refer to Web version on PubMed Central for supplementary material.

Acknowledgments

We thank Dr. Amy Harms for performing the ESI-MS analysis and Grzegorz Sabat for performing the protease digestion and MS analysis of ZmaA-AT. We also thank Angela Podevels for technical assistance in cloning one of the *zmaA*-ACP1 constructs.

ABBREVATIONS

ACP	acyl carrier protein
NRPS	nonribosomal peptide synthetase
PKS	polyketide synthase
1,3-bPG	1,3-bisphospho-D-glycerate
AT	acyltransferase
KS	ketosynthase
ER	enoylreductase
DH	dehydratase
C	condensation

REFERENCES

1. Cane DE, Walsh CT, Khosla C. Harnessing the biosynthetic code: combinations, permutations, and mutations. Science 1998;282:63–68. [PubMed: 9756477]
2. Staunton J, Weissman KJ. Polyketide biosynthesis: a millennium review. Nat. Prod. Rep 2001;18:380–416. [PubMed: 11548049]
3. Khosla C, Gokhale RS, Jacobsen JR, Cane DE. Tolerance and specificity of polyketide synthases. Annu. Rev. Biochem 1999;68:219–253. [PubMed: 10872449]
4. Fujimori DG, Walsh CT. What's new in enzymatic halogenations. Curr. Opin. Chem. Biol 2007;11:553–560. [PubMed: 17881282]
5. Walsh CT. Combinatorial biosynthesis of antibiotics: Challenges and opportunities. ChemBioChem 2002;3:124–134.
6. Moore BS, Hertweck C. Biosynthesis and attachment of novel bacterial polyketide synthase starter units. Nat. Prod. Rep 2002;19:70–99. [PubMed: 11902441]
7. Chan YA, Podevels AM, Kevany BM, Thomas MG. Biosynthesis of polyketide synthase extender units. Nat. Prod. Rep 2009;26:90–114. [PubMed: 19374124]

8. Liu Y, Hazzard C, Eustaquio AS, Reynolds KA, Moore BS. Biosynthesis of salinosporamides from alpha,beta-unsaturated fatty acids: implications for extending polyketide synthase diversity. J. Am. Chem. Soc 2009;131:10376–10377. [PubMed: 19601645]
9. Wu K, Chung L, Revill P, Katz L, Reeves CD. The FK520 gene cluster of *Streptomyces hygroscopicus* var. *ascomyceticus* (ATCC14891) contains genes for biosynthesis of unusual polyketide extender units. Gene 2000;251:81–90. [PubMed: 10863099]
10. Yu T-W, Bai L, Clade D, Hoffman D, Toelzer S, Trinh KQ, Xu J, Moss SJ, Leistner E, Floss HG. The biosynthetic gene cluster of the maytansinoid antitumor agent ansamitocin from *Actinosynnema pretiosum*. Proc. Natl. Acad. Sci. USA 2002;99
11. Ligon J, Hill S, Beck J, Zirkle R, Molnar I, Zawodny J, Money S, Schupp T. Characterization of the biosynthetic gene cluster for the antifungal polyketide soraphen A from *Sorangium cellulosum* So ce26. Gene 2002;285:257–267. [PubMed: 12039053]
12. Chan YA, Boyne MT II, Podevels AM, Klimowicz AK, Handelsman J, Kelleher NL, Thomas MG. Hydroxymalonyl-acyl carrier protein (ACP) and aminomalonyl-ACP are two additional type I polyketide synthase extender units. Proc. Natl. Acad. Sci. USA 2006;103:14349–14354. [PubMed: 16983083]
13. Rachid S, Scharfe M, Blöcker H, Weissman KJ, Müller R. Unusual chemistry in the biosynthesis of the antibiotic chondrochlorens. Chem. Biol 2009;16:70–81. [PubMed: 19171307]
14. Broderick NA, Goodman RM, Raffa KF, Handelsman J. Synergy between zwittermicin A and *Bacillus thuringiensis* subsp. *kurstaki* against gypsy moth (Lepidoptera: Lymantriidae). Environ. Entomol 2000;29:101–107.
15. Silo-Suh LA, Lethbridge BJ, Raffel SJ, He H, Clardy J, Handelsman J. Biological activities of two fungistatic antibiotics produced by *Bacillus cereus* UW85. Appl. Environ. Microbiol 1994;60:2023–2030. [PubMed: 8031096]
16. Silo-Suh LA, Stabb EV, Raffel SJ, Handelsman J. Target range of zwittermicin A, an aminopolyol antibiotic from Bacillus cereus. Curr. Microbiol 1998;37:6–11. [PubMed: 9625782]
17. Kato Y, Bai L, Xue Q, Revill WP, Yu T-W, Floss HG. Functional expression of genes involved in the biosynthesis of the novel polyketide chain extension unit, methoxymalonyl-acyl carrier protein, and engineered biosynthesis of 2-desmethyl-2-methoxy-6-deoxyerythronolide B. J. Am. Chem. Soc 2002;124:5268–5269. [PubMed: 11996558]
18. Ruan X, Pereda A, Stassi DL, Zeidner D, Summers RG, Jackson M, Shivakumar A, Kakavas S, Staver MJ, Donadio S, Katz L. Acyltransferase domain substitutions in erythromycin polyketide synthase yield novel erythromycin derivatives. J. Bacteriol 1997;179:6416–6425. [PubMed: 9335291]
19. Emmert EAB, Klimowicz AK, Thomas MG, Handelsman J. Genetics of zwittermicin A production by *Bacillus cereus*. Appl. Environ. Microbiol 2004;70:104–113. [PubMed: 14711631]
20. Kevany BM, Rasko DA, Thomas MG. Characterization of the complete zwittermicin A biosynthesis gene cluster from *Bacillus cereus*. Appl. Environ. Microbiol 2009;75:1144–1155. [PubMed: 19098220]
21. Cheng YQ, Tang GL, Shen B. Type I polyketide synthase requiring a discrete acyltransferase for polyketide biosynthesis. Proc. Natl. Acad. Sci. USA 2003;100:3149–3154. [PubMed: 12598647]
22. Chan YA, Thomas MG. Formation and characterization of acyl carrier protein-linked polyketide synthase extender units. Methods Enzymol 2009;459:143–163. [PubMed: 19362639]
23. Liou GF, Lau J, Cane DE, Khosla C. Quantitative analysis of loading and extender unit acyltransferases of modular polyketide synthases. Biochemistry 2003;42:200–207. [PubMed: 12515555]
24. Joshi VC. Mechanism of malonyl-coenzyme A-acyl carrier protein transacylase. Biochem. J 1972;128:43–44.
25. Keatinge-Clay AT, Shelat AA, Savage DF, Tsai S-C, Miercke LJW, O'Connell JD III, Khosla C, Stroud RM. Catalysis, specificity, and ACP docking site of *Streptomyces coelicolor* malonyl-CoA:ACP transacylase. Structure 2003;11:147–154. [PubMed: 12575934]
26. Reeves CD, Chung LM, Liu Y, Xue Q, Carney JR, Revill WP, Katz L. A new substrate specificity for acyl transferase domains of the ascomycin polyketide synthase in *Streptomyces hygroscopicus*. J. Biol. Chem 2002;277:9155–9159. [PubMed: 11786554]

27. Roujeinikova A, Simon WJ, Gilroy J, Rice DW, Rafferty JB, Slabas AR. Structural studies of fatty acyl-(acyl carrier protein) thioesters reveal a hydrophobic binding cavity that can expand to fit longer substrates. J. Mol. Biol 2007;365:135–145. [PubMed: 17059829]

28. Lopanik NB, Shields JA, Bucholz TJ, Rath CM, Hothersall J, Haygood MG, Häkansson K, Thomas CM, Sherman DH. In vivo and in vitro transacylation by BryP, the putative bryostatin pathway acyltransferase derived from an uncultured marine symbiont. Chem. Biol 2008;15:1175–1186. [PubMed: 19022178]

29. Tang GL, Cheng YQ, Shen B. Leinamycin biosynthesis revealing unprecedented architectural complexity for a hybrid polyketide synthase and nonribosomal peptide synthetase. Chem. Biol 2004;11:33–45. [PubMed: 15112993]

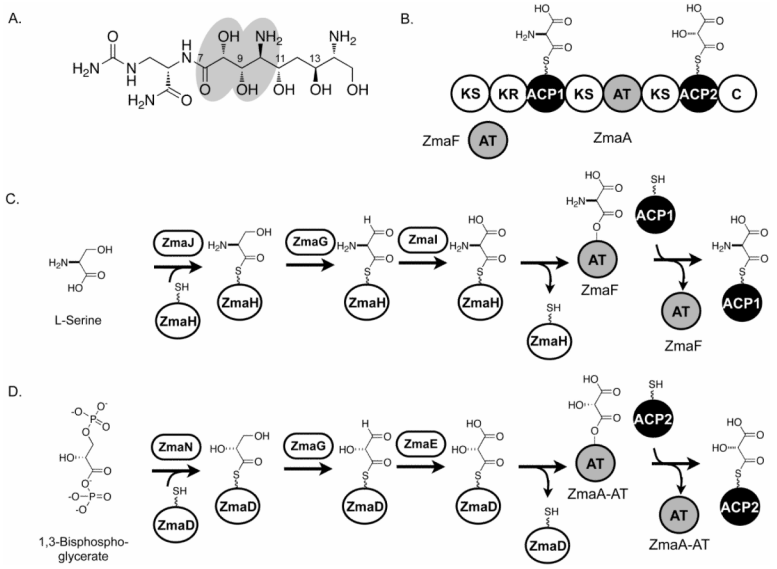

Figure 1.

Incorporation of two ACP-linked PKS extender units in zwittermicin A biosynthesis. (A) Structure of zwittermicin A with glycyl and glycolyl moieties highlighted. These moieties are derived from the incorporation of (2*S*)-aminomalonyl-ZmaH and (2*R*)-hydroxymalonyl-ZmaD, respectively. (B) Schematic of the domain architecture of the enzymes involved in (2*S*)-aminomalonyl-ACP and (2*R*)-hydroxymalonyl-ACP incorporation. The specific domains characterized are highlighted in grey (AT domains) and black (ACP domains). (C) Schematic of the enzymes and domains involved in the conversion of L-serine to (2*S*)-aminomalonyl-ACP1. The transacylation reaction catalyzed by ZmaF is shown in two half-reactions with the first half-reaction involving the formation of a (2*S*)-aminomalonyl-O-ZmaF intermediate followed by the second half-reaction to generate (2*S*)-aminomalonyl-ACP1. (D) Schematic of the enzymes and domains involved in the formation of (2*R*)-hydroxymalonyl-ACP2. The two half-reactions of the ZmaA-AT reactions are also shown. The squiggles denote the 4′-Ppant prosthetic groups of the ACPs. The discrete AT (ZmaF) and the embedded AT (ZmaA-AT) are shown in gray, and the ACPs of ZmaA are shown in black. For our analysis, ZmaA-ACP1, ZmaA-ACP2, and ZmaA-AT were excised from ZmaA.

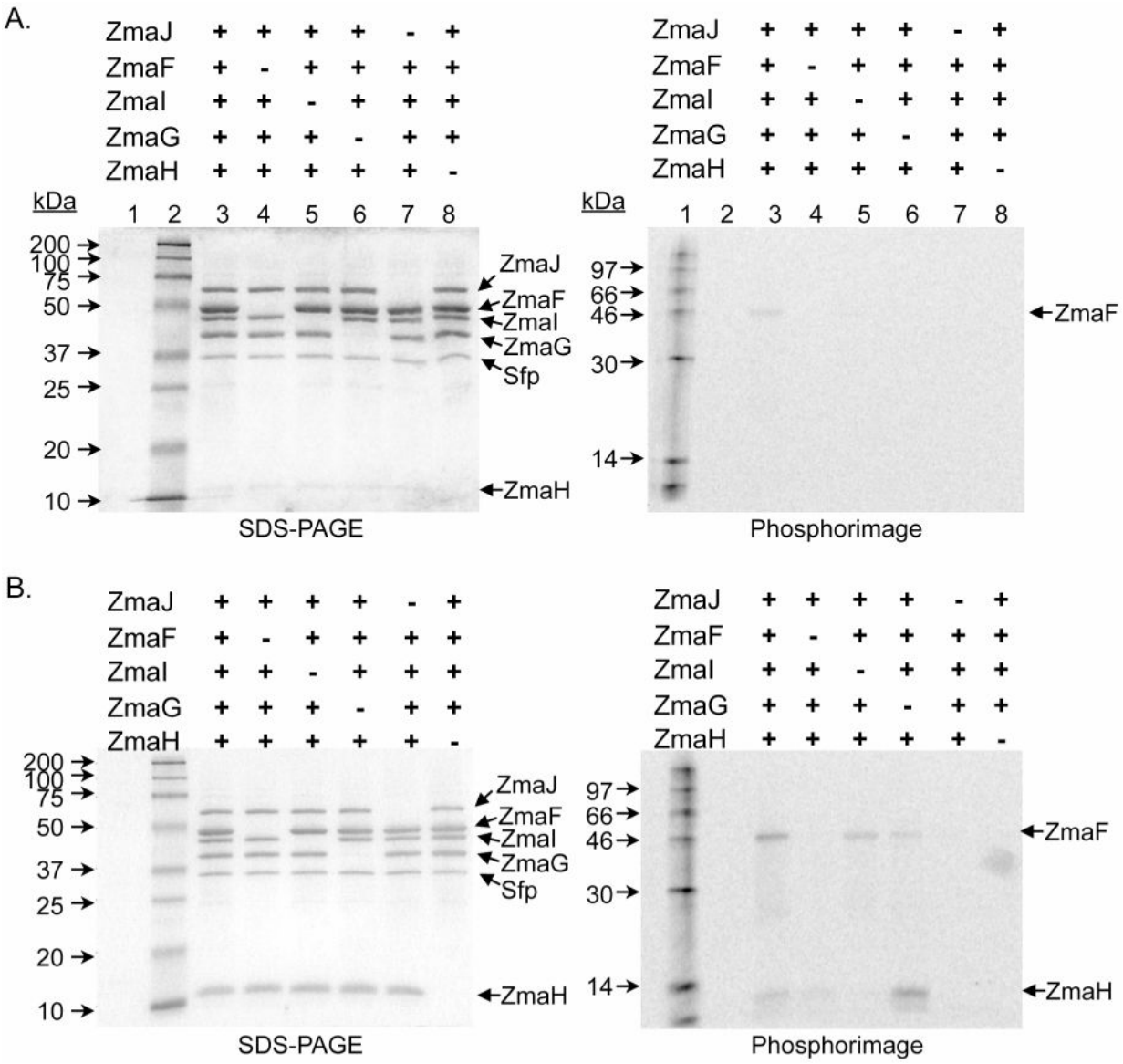

Figure 2.

Transacylase assay of ZmaF using [^{14}C]-(2*S*)-aminomalonyl-ZmaH at (A) low concentrations of ZmaH (1.25 μM) or (B) high concentrations of ZmaH (5 μM). SDS-PAGE/Coomassie blue analysis of reaction mixtures and corresponding phosphorimage. Pluses and minuses denote presence/absence of corresponding enzyme for each reaction mixture. The radiolabeled molecular weight marker was loaded in lane 1, and the standard molecular mass marker was loaded in lane 2.

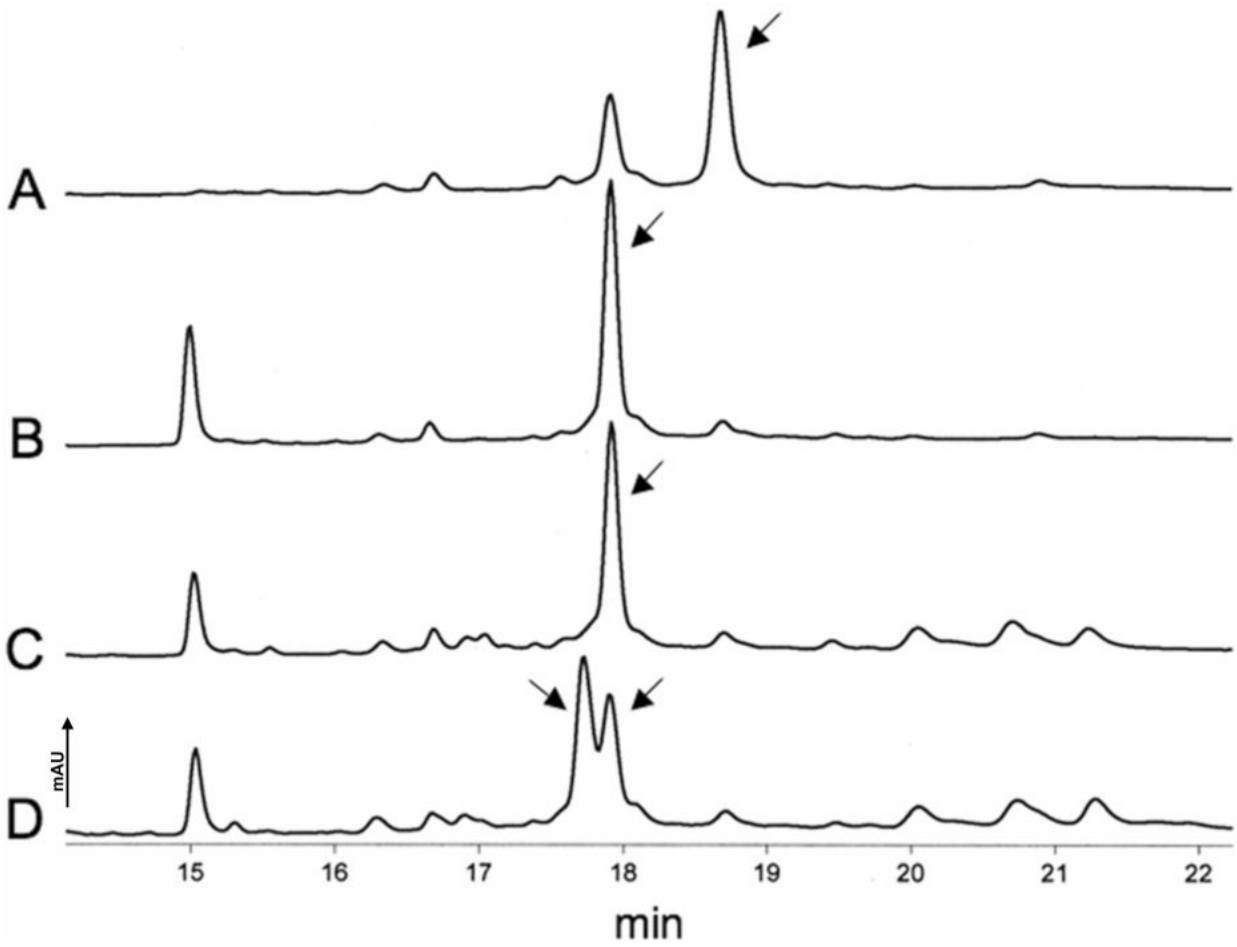

Figure 3.
HPLC analysis of ZmaA-ACP1 using C18 peptide column. Arrows identify the peaks associated with the ZmaA-ACP1 derivatives, which were collected and analyzed by MS. The y-axis is milliabsorption units (mAU); the x-axis noting the minutes of elution. Reactions contain (A) apo-ZmaA-ACP1; (B) apo-ZmaA-ACP1, Sfp; (C) apo-ZmaA-ACP1, Sfp, ZmaH, ZmaJ, ZmaG, ZmaI; (D) apo-ZmaA-ACP1, Sfp, ZmaH, ZmaJ, ZmaG, ZmaI, ZmaF.

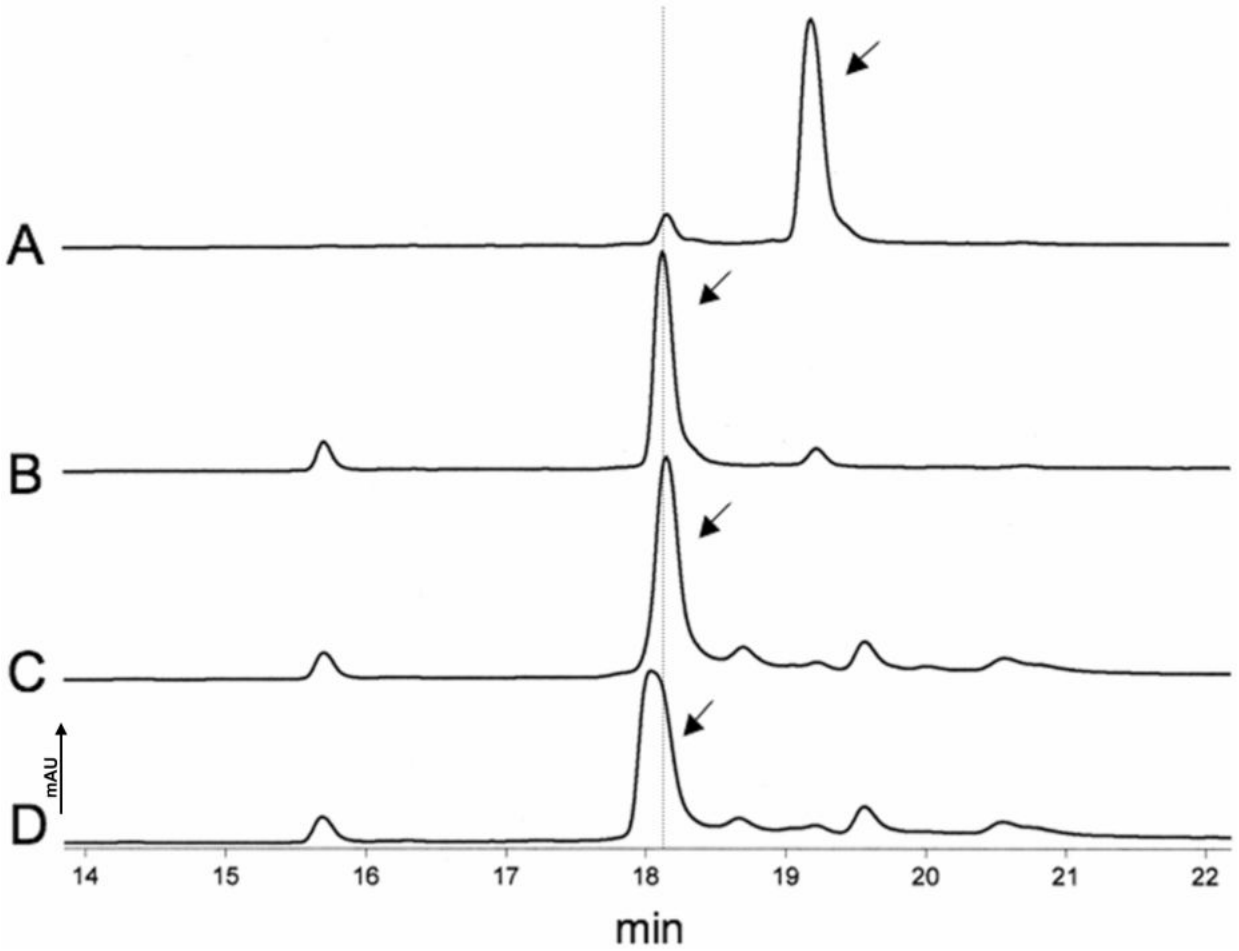

Figure 4.
HPLC analysis of ZmaA-ACP2 using C18 peptide column. Arrows identify the peaks associated with the ZmaA-ACP2 derivatives, which were collected and analyzed by MS. The y-axis denotes milliabsorption units (mAU); the x-axis denotes elution time. Reactions contain (A) apo-ZmaA-ACP2; (B) apo-ZmaA-ACP2, Sfp; (C) apo-ZmaA-ACP2, Sfp, ZmaD, ZmaN, ZmaG, ZmaE; (D) apo-ZmaA-ACP2, Sfp, ZmaD, ZmaN, ZmaG, ZmaE, ZmaA-AT. The vertical line is aligned with the elution of holo-ZmaA-ACP2.

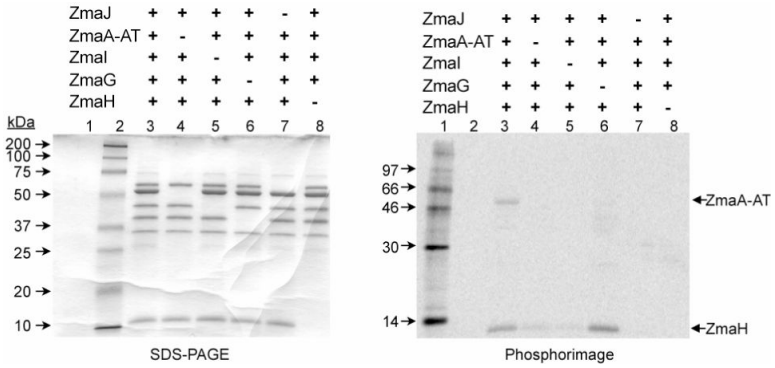

Figure 5.

Transacylase assay of ZmaA-AT using [^{14}C]-(2*S*)-aminomalonyl-ZmaH at high concentrations of ZmaH (5 μM). SDS-PAGE/Coomassie blue analysis of reaction mixtures and corresponding phosphorimage. Pluses and minuses denote presence/absence of corresponding enzyme for each reaction mixture. The radiolabeled molecular weight marker was loaded in lane 1, and the standard molecular mass marker was loaded in lane 2.

Table 1

Mass spectrometry analysis of purified ZmaA-ACP1 species

	ZmaA-ACP1 Species[a]					
	apo-	**holo-**	**amino-malonyl-**	**glycyl-**	**2-amino-3-oxopropionyl-**	**2-amino-3,3-dihydroxy-propionyl-**
Theoretical [M+H]$^{+}$[b]	**19,090**	**19,429**	**19,531**	**19,487**	**19,515**	**19,533**
Reaction	**Experimental [M+H]$^{+}$**					
Apo-ZmaA-ACP1	19,085	-	-	-	-	-
Holo-ZmaA-ACP1	-	19,425	-	-	-	-
Complete	-	19,434	-	19,487	-	-
No ZmaF	-	19,425	-	-	-	-
No ZmaI	-	19,425	-	-	19,514	
		19,428[c]			19,518[c]	

[a] Masses are in Daltons. Masses were determined by MALDI-TOF MS unless otherwise noted.

[b] The theoretical masses are based on removal of the N-terminal methionine residue.

[c] Mass determined by ESI-MS

Biochemistry. Author manuscript; available in PMC 2011 May 4.

Table 2

Mass spectrometry analysis of purified ZmaA-ACP1 species

	ZmaA-ACP1 Species			
	apo-	**holo-**	**hydroxy-malonyl-**	**glycolyl-**
Theoretical $[M+H]^{+}$ *b*	**21,522**	**21,861**	**21,963**	**21,920**
Reaction	**Experimental $[M+H]^{+}$**			
Apo-ZmaA-ACP2	21,522	-	-	-
Holo-ZmaA-ACP2	-	21,858	-	-
Complete	-	-	-	21,911
No ZmaA-AT	-	21,852	-	-

a Masses are in Daltons. Masses were determined by MALDI-TOF MS.

b The theoretical masses are based on removal of the N-terminal methionine residue.